iScience

CellPress
OPEN ACCESS

Article

Direct interspecies electron transfer enables anaerobic oxidation of sulfide to elemental sulfur coupled with CO_2-reducing methanogenesis

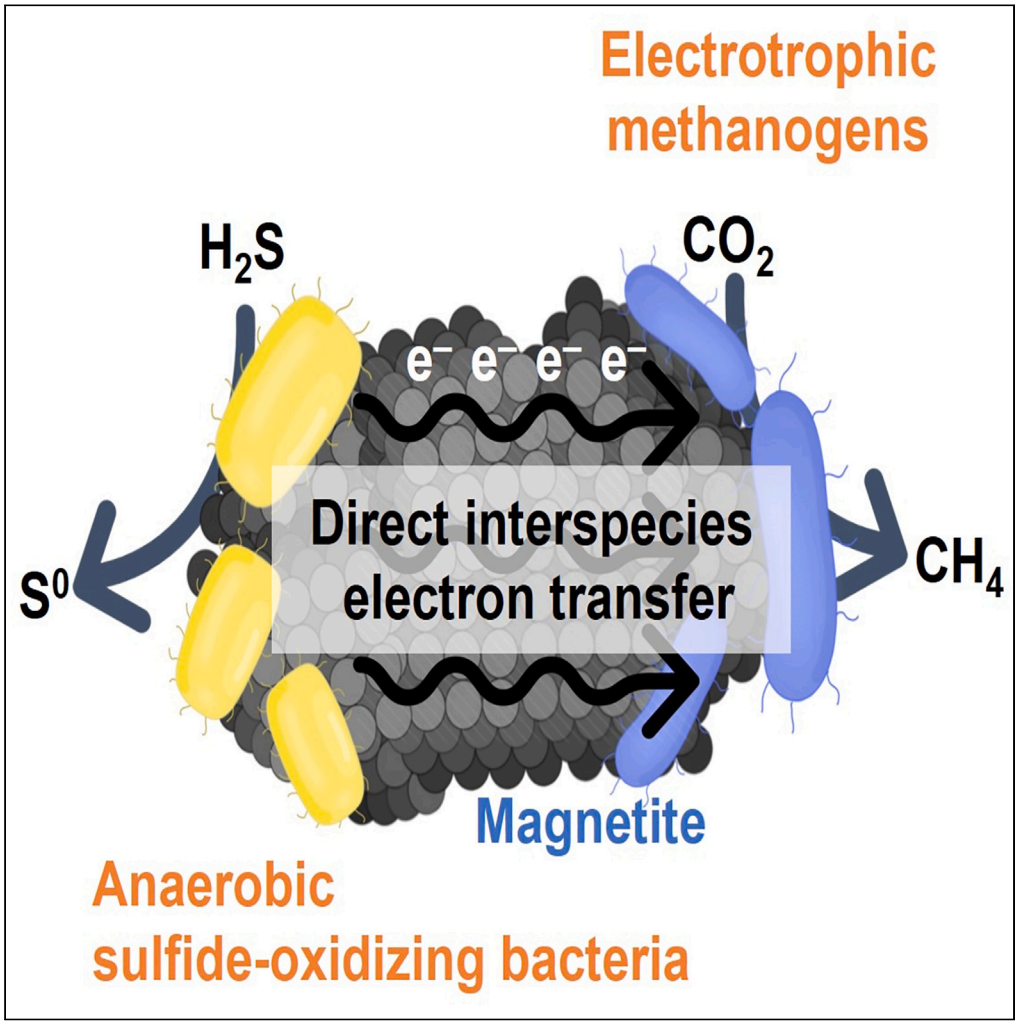

Heejung Jung, Hyeonjung Yu, Changsoo Lee

cslee@unist.ac.kr

Highlights

Magnetite supplementation completely removed H_2S in biogas from sulfur-rich waste AD

S^0 accumulated in the presence of magnetite and CO_2-reducing methanogenic activity

DIET-coupling of sulfide oxidation to electrotrophic methanogenesis was confirmed

A new electric syntrophy between ASOBs and electrotrophic *Methanothrix* is proposed

Jung et al., iScience *26*, 107504
September 15, 2023
https://doi.org/10.1016/j.isci.2023.107504

iScience

CellPress
OPEN ACCESS

Article

Direct interspecies electron transfer enables anaerobic oxidation of sulfide to elemental sulfur coupled with CO_2-reducing methanogenesis

Heejung Jung,[1,3,4] Hyeonjung Yu,[1] and Changsoo Lee[1,2,5,*]

SUMMARY

Electric syntrophy between fatty acid oxidizers and methanogens through direct interspecies electron transfer (DIET) is essential for balancing acidogenesis and methanogenesis in anaerobic digestion. Promoting DIET using electrically conductive additives proved effective in enhancing methanogenesis; however, its possibility to affect other microbial redox reactions in methanogenic systems has been little studied. This study provides the first confirmation of the electro-syntrophic coupling of sulfide oxidation to S^0 with CO_2-reducing methanogenesis in sulfur-rich methanogenic cultures supplemented with conductive magnetite (100–700-nm particle size). The H_2S content in biogas, initially exceeding 5000 ppmv, decreased to below 1 ppmv along with an accumulation of extracellular S^0 (60–70 mg/L; initially <1 mg/L) at a magnetite dose of 20 mM Fe, while there were no significant changes in methane yield. A comprehensive polyphasic approach demonstrated that the S^0 formation occurs through electro-syntrophic oxidation of sulfide coupled with CO_2-reducing methanogenesis, involving *Methanothrix* as the dominant methanogen.

INTRODUCTION

Converting organic waste into methane-rich biogas through anaerobic digestion (AD) is a key process for sustainable waste management and is receiving increasing attention as a viable source of renewable energy. One of the most exciting recent findings in the field of AD is the electric syntrophy between exoelectrogenic bacteria and electrotrophic methanogens via direct interspecies electron transfer (DIET).[1–3] DIET is considered energetically and kinetically more favorable than conventionally known indirect interspecies electron transfer (IIET), which is mediated by electron-rich metabolites, such as hydrogen or formate,[4] although they both play a crucial role in the methanogenic degradation of fermentation products, such as volatile fatty acids (VFAs) and ethanol.[5] An imbalance between the production and consumption of fermentation products leads to digester souring (i.e., a sudden pH drop with an accumulation of acids) and even failure. Therefore, efficient syntrophic methanogenesis via interspecies electron transfer is essential for the stabilization of and energy recovery from organic matter through AD.

DIET does not require complex enzymatic steps for producing and utilizing H_2 or formate that is necessary for IIET, and is not inhibited by increased hydrogen partial pressure.[4,5] Accordingly, the possibility has been raised that the methanogenic degradation of fermentation products may be improved by promoting DIET.[5] In support of this hypothesis, Kato et al.[2] first reported in 2012 the acceleration of methanogenesis by the addition of (semi)conductive iron oxides in rice paddy soil enrichments. The authors suggested that (semi)conductive iron oxides could promote the electric syntrophy between *Geobacter* and *Methanosarcina* by serving as conduits for DIET. Subsequently, many studies have demonstrated the effectiveness of adding conductive materials (mostly carbon- or iron-based) in promoting DIET and thus accelerating methanogenesis in different AD processes.[5–7] DIET via abiotic conductive materials bypasses the need for cell-to-cell electrical contacts via biological components, such as outer membrane cytochromes and conductive pili (e-pili), necessary for biological DIET,[8] which makes adding conductive materials a simple and efficient approach to promote DIET. These findings presented new possibilities for improving the methanogenic performance and stability of anaerobic digesters.

[1]Department of Urban and Environmental Engineering, Ulsan National Institute of Science and Technology (UNIST), 50 UNIST-gil, Eonyang-eup, Ulju-gun, Ulsan 44919, Republic of Korea

[2]Graduate School of Carbon Neutrality, Ulsan National Institute of Science and Technology (UNIST), 50 UNIST-gil, Eonyang-eup, Ulju-gun, Ulsan 44919, Republic of Korea

[3]Present address: Department of Chemical Engineering, Columbia University, New York, NY, USA

[4]Lead contact

[5]Present address: Geologic Environment Research Division, Korea Institute of Geoscience and Mineral Resources (KIGAM), Daejeon 34132, Republic of Korea

*Correspondence: cslee@unist.ac.kr

https://doi.org/10.1016/j.isci.2023.107504

Our understanding of the role and mechanism of DIET in methanogenic environments has advanced significantly over the last decade, and engineering DIET using conductive additives is now considered a promising strategy to boost AD,[7] although performance improvement may not be due solely to the promotion of DIET.[9] Studies on the effects of conductive additives in mixed-culture AD processes have thus far focused almost exclusively on the enhancement of methane production and the microbial reactions involved in electro-syntrophic methanogenesis. However, given that electroactive microorganisms are commonly present in different anaerobic environments, including anaerobic digesters,[10,11] conductive additives could also affect, either directly (i.e., promoting electric syntrophy) or indirectly (i.e., altering electron flow), microbial redox reactions other than those involved in methane production in AD processes.[12] Therefore, it is likely that the effect of conductive additives on electron flow in methanogenic microbial communities will be complex, particularly when electron sinks other than methanogenesis are abundant. Although changes in electron flow directly influence the performance of anaerobic digesters, these changes and their implications have been studied very little to date.

In a recent study, we investigated the effect of adding magnetite (Fe_3O_4), a commonly used conductive material for promoting DIET, during continuous AD of a sulfur-rich waste mixture and observed no apparent enhancement of methane production.[12] Instead, we found that sulfide produced by dissimilatory sulfate reduction was biologically oxidized to elemental sulfur (S^0) and accumulated extracellularly in the presence of magnetite, resulting in a significant reduction in the H_2S content in biogas. This novel finding offers a new perspective for *in situ* H_2S removal and S^0 recovery in digesters, which are of particular interest in the management of AD plants. H_2S inhibits methanogenesis and causes odor and corrosion problems, and therefore the control of H_2S formation and emission is important for stable AD.[13,14] Furthermore, the H_2S content in biogas (usually from several hundred to several thousand ppmv) must be reduced by a costly gas-cleaning process to meet the standards for different uses of biogas.[15] Based on molecular, electrochemical, and thermodynamic analyses, we proposed a novel electric syntrophy between anaerobic microbial sulfide oxidation to S^0 and methanogenic reduction of CO_2 via magnetite-mediated DIET. Given that naturally occurring conductive minerals, such as metal ores, are abundant in nature, the proposed electric syntrophy may be a new type of sulfur metabolism in anaerobic environments, playing a significant role in the global sulfur cycle. Although strong circumstantial evidence was provided, direct evidence for the proposed electric syntrophy was not obtained in our previous study, which focused primarily on the formation of extracellular S^0. Recently, Jiao et al.[16] also proposed an electric syntrophy between sulfide-oxidizing bacteria and methanogens through pyrite (FeS_2)-mediated DIET in batch AD of sewage sludge based on the metagenome-assembled genomes recovered from the digesters. Although the genetic potential of sulfide-oxidizing bacteria to participate in DIET was suggested, direct experimental evidence for the proposed DIET-based syntrophy was not provided.

Therefore, the present study aimed to substantiate the electro-syntrophic coupling of sulfide oxidation to electrotrophic methanogenesis in the presence of magnetite during the AD of a waste mixture of sulfur-rich macroalgal biomass and cheese whey (Figure 1). The accumulation of extracellular S^0 from the microbial oxidation of sulfide was reproduced in duplicate lab-scale digesters, and the proposed electric syntrophy was verified by a series of semi-continuous cultures with the digester slurry. This is the first study to show an electro-syntrophic association between anaerobic sulfide oxidation to S^0 and electrotrophic methanogenesis from CO_2. The findings of this study not only advance our understanding of electro-syntrophic microbial metabolisms in methanogenic environments but also help to improve strategies for engineering DIET in AD processes for enhanced energy recovery and process stability.

RESULTS AND DISCUSSION

H_2S removal and S^0 formation

Duplicate anaerobic continuously stirred tank reactors (RM1 and RM2) showed very similar reaction profiles with stable organic removal and methane production across the experimental phases with increasing doses (Phases M0, M8 and M20 at 0, 8 and 20 mM Fe, respectively) of magnetite (100–700-nm particle size) (Table 1; Figure 2). In line with our previous observation,[12] magnetite addition had no significant effect on methane production but substantially reduced H_2S production in both reactors. The methane yield remained consistent regardless of the magnetite dose at 0.24–0.25 L/g chemical oxygen demand (COD) fed, corresponding to around 0.37 L/g COD removed, which is close to the theoretical yield of 0.35 L/g COD removed. This indicates that methanogenesis was active and the primary electron sink in the reactors throughout the experiment. The H_2S content in biogas was over 5,200 ppmv in Phase M0, which is within

1) Lab-scale anaerobic digesters operated with magnetite addition

Research questions

- Does magnetite addition affect microbial redox reactions other than methanogenesis during AD?
- How does DIET promotion influence the fate of sulfur species in sulfur-rich methanogenic cultures?

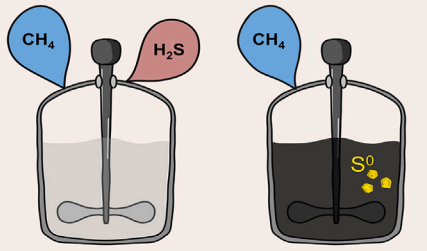

Key measures

- CH_4 and H_2S productions
- Sulfide and extracellular S^0 concentrations
- Electron transport system activity
- Microbial community structure (electroactive microorganisms)
- Residual magnetite concentration
- Cyclic voltammetric behavior (redox reactions)

2) Semi-continuous cultures with or without magnetite and methanogenic inhibitors

Research questions

- Is DIET-based electric syntrophy necessary for the oxidation of sulfide to elemental sulfur?
- What reduction reaction is coupled with sulfide oxidation to drive the electric syntrophy?

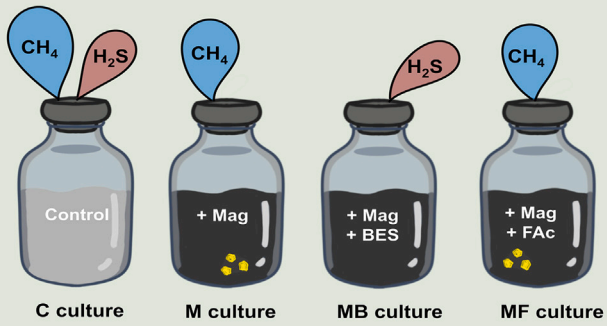

Key measures

- CH_4 and H_2S productions
- Sulfide and extracellular S^0 concentrations

3) Stable isotope probing experiment using [^{13}C]bicarbonate

Research questions

- Dose the electrotrophic conversion of CO_2 to CH_4 provide syntrophic support for the oxidation of sulfide to S^0?
- What electrotrophic methanogen participates in the syntrophic relationship?

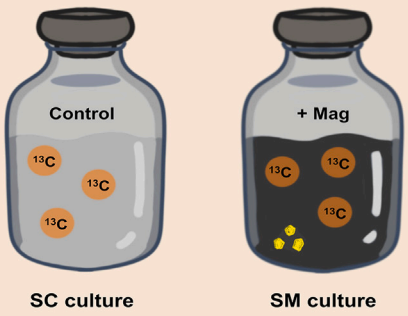

Key measures

- CH_4 and H_2S productions
- Sulfide and extracellular S^0 concentrations
- ^{13}C- and ^{12}C-labelled archaeal community composition

Figure 1. Overview of the experimental flow and key research questions

DIET, direct interspecies electron transfer; Mag, magnetite; BES, 2-bromoethanesulfonate (to inhibit all methanogenic pathways); FAc, fluoroacetate (to selectively inhibit aceticlastic methanogenesis).

Table 1. Steady-state process performance data for each experimental phase

		Phase M0		Phase M8		Phase M20	
Process parameter	Unit	RM1	RM2	RM1	RM2	RM1	RM2
COD removal	%	66.3 (11.4)[a]	64.1 (22.7)	62.6 (10.5)	63.2 (9.2)	66.0 (25.7)	65.9 (21.1)
Residual VFAs	mg COD/L	10.9 (1.4)	9.12 (0.7)	ND[b,*]	ND*	ND*	ND*
CH_4 production rate	mL/L·d	68.9 (7.0)	68.3 (4.2)	68.1 (8.9)	67.5 (7.8)	64.8 (2.6)	64.0 (3.1)
CH_4 yield	L/g COD fed	0.25 (0.01)	0.25 (0.01)	0.25 (0.02)	0.25 (0.01)	0.24 (0.0)	0.24 (0.01)
CH_4 yield	L/g COD removed	0.38 (0.1)	0.38 (0.0)	0.38 (0.1)	0.37 (0.1)	0.37 (0.0)	0.37 (0.0)
H_2S production rate	mL/L·d	0.043 (0.01)	0.046 (0.0)	0.005 (0.0)*	0.004 (0.0)*	<0.001*	<0.001*
H_2S content in biogas	ppmv	5,283 (683)	5,217 (161)	553 (49)*	484 (42)*	<1*,#	<1*,#
Total dissolved sulfide	mg S/L	58.1 (4.4)	57.5 (3.2)	58.9 (6.2)	61.6 (1.2)	58.6 (1.1)	55.4 (4.3)
Extracellular S^0	mg/L	<1	<1	69.2 (1.3)*	69.9 (0.5)*	63.3 (2.0)*	61.9 (8.0)*
Residual magnetite	mM Fe	ND	ND	8.5 (0.1)	8.2 (0.0)	19.7 (0.3)	23.4 (0.5)

Symbols indicate statistically significant differences ($p < 0.05$) compared to Phase M0 (*) and to Phase M8 (#).
[a]Standard deviation represents in parenthesis.
[b]Not detected.

the typical range of 0.1–2% (v/v) depending on substrate composition but too high for use in engines or vehicles (<1–1000 ppmv).[17] With the addition of magnetite, the H_2S content fell drastically to around 500 ppmv in Phase M8 and further below 1 ppmv in Phase M20. Meanwhile, the residual concentration of total dissolved sulfide (TDS) remained around 60 mg S/L across the experimental phases (Table 1), which is lower than the inhibitory concentration to methanogens (100–800 mg/L).[17] These results suggest that the reduced H_2S production in the presence of magnetite was not due to the suppression of dissimilatory sulfate reduction but rather to the removal of produced sulfide. It should be noted that, in Phases M8 and M20, there was an accumulation of extracellular S^0 (61.9–69.9 mg/L) without detectable formation of FeS (<0.1 mg Fe/L), indicating that H_2S was not removed by FeS precipitation but rather through the oxidation of sulfide to S^0 under magnetite-added conditions. Supporting this observation, the results of cyclic voltammetry (CV) of Phase M20 biomass in RM1, cultivated for 24 h using acetate and sulfate as the sole carbon and sulfur sources, showed a pair of anodic and cathodic peaks (+0.37 and −0.02 V vs. Ag/AgCl) corresponding to the redox reactions between (poly)sulfide and S^0 (Figure S1).[18] In contrast, no peaks relevant to these redox reactions were detected in the cyclic voltammogram of the Phase M0 biomass, further evidencing the essential role of magnetite in mediating these reactions. The experimental results summarized above, which agree with our previous study,[12] reconfirm the oxidation of sulfide to extracellular S^0 in the presence of magnetite under methanogenic conditions.

Microbial sulfide oxidation to S^0

Anaerobic batch experiments using the same inoculum sludge as for RM1 and RM2 were performed with sodium acetate (5 g COD/L) to determine whether the oxidation of sulfide to S^0 is biological or chemical. The experiments were carried out with or without the addition of magnetite, under biotic and abiotic (autoclaved sludge or no inoculation) conditions. During 28 days of cultivation, a noticeable formation of extracellular S^0 was observed only in the biotic cultures dosed with magnetite (20 mM Fe), and the S^0 accumulation was significantly lower when sodium sulfide was added as the sulfur source (11.2 mg S/L) than when sodium sulfate was added (67.5 mg S/L). The difference in S^0 accumulation could be attributed to the volatilization loss of H_2S in the former, especially during the initial period of incubation, when the sulfide concentration is high. The calculated H_2S to HS^- ratio at equilibrium (pKa = 6.76 at 37°C,[19]) was approximately 8% in the cultures (initial pH of 7.87), and therefore a considerable amount of sulfide in the medium must have been released as H_2S into the gas phase during the incubation of the cultures with sodium sulfide. Meanwhile, no detectable amount of S^0 (<1 mg/L) formed in any abiotic culture regardless of the presence or absence of magnetite. These results indicate that the magnetite-aided sulfide oxidation to S^0 was microbially mediated rather than through chemical reactions between sulfide and magnetite,[20] which agrees with our previous observation.[12] Accordingly, the residual magnetite concentration remained unchanged from the dosed levels throughout the experiment in the duplicate reactors (Table 1), and the X-ray diffraction (XRD) profiles of the reactor samples taken on Day 525 (Phase M20) matched that of

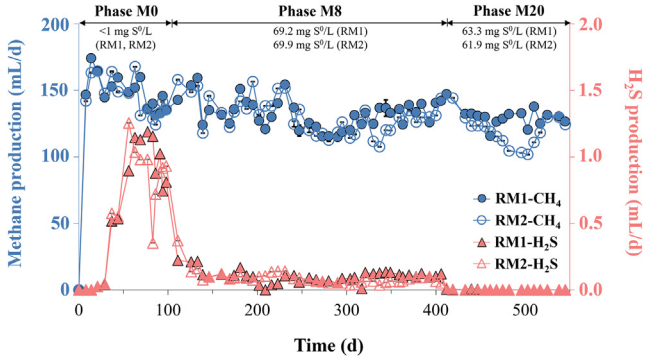

Figure 2. Methane and H_2S production profiles of duplicate reactors RM1 and RM2

The reactors were operated at increasing magnetite concentrations (Phases M0, M8, and M20 at 0, 8, and 20 mM Fe, respectively). The average extracellular S^0 concentrations of the reactors for each experimental phase under steady-state conditions are presented. Error bars represent standard deviations of duplicate measurements.

pure magnetite (Figure S2). These results show that the added magnetite remained intact with no significant dissolution or chemical transformation during the reactor operation.

The microscopic examination of the reactor samples revealed that magnetite particles and microorganisms agglomerated to form flock-like aggregates, in comparison with the bare carbon tape where the specimen was loaded (Figures 3A and S3). Several previous studies on DIET-promoted AD using submicron magnetite particles have reported the formation of conductive cell-magnetite aggregates,[12,21,22] which shortens the distance between syntrophic partners involved in various microbial redox reactions in methanogenic systems and facilitates their electron exchange.[5,23] Additionally, magnetite can compensate for the lack of e-pili and *c*-type cytochromes in extracellular electron exchange[24] and can facilitate DIET even between microorganisms lacking these biological connectors.[3,25,26] Accordingly, the electron transport system (ETS) activity increased more than 3-fold, from approximately 4 to over 12 μg/mL•min, in both RM1 and RM2 with the addition of magnetite (Figure 3B). Comparable levels of ETS activity increase have been reported in other studied using conductive additives to promote DIET in AD.[27,28] ETS activity is an indicator of microbial respiration and redox reactions, which has been shown to increase under DIET-promoting conditions with magnetite addition.[29–32] Taken together, magnetite did not act as an electron shuttle but likely provided cell-to-cell electrical connections for syntrophic sulfide oxidation to S^0 in the duplicate reactors. Fluorescence microscopy with a sulfane sulfur–specific probe, SSP4, confirmed the extracellular deposition of S^0 in proximity to cell-magnetite aggregates (Figure 3C), supporting the conversion of sulfide to S^0 via extracellular electron transfer.

Microbial responses to magnetite addition

High-throughput sequencing (HTS) was performed to investigate the effects of magnetite addition on the microbial communities in the experimental reactors. A total of 104,133 reads were obtained from rRNA (i.e., cDNA) libraries, and they were clustered into 398 operational taxonomic units (OTUs; 381 bacterial and 17 archaeal). The taxonomic affiliations of major OTUs (>2% of the total bacterial or archaeal reads in at least one sample) are presented in Figure 4. The microbial community structures of the reactors changed greatly with the addition of magnetite, as seen in the bacterial and archaeal cluster dendrograms generated from the distribution of OTUs, where the community structures in Phase M0 were clustered remotely from those in Phases M8 and M20 (Figure 5). Twenty-three phyla were identified from the bacterial sequences, with *Bacteroidetes*, *Proteobacteria*, and *Spirochaetes* being the dominant phyla, and 28 sequences (28 OTUs) were unclassified at the phylum level. Changes in bacterial community structure after adding magnetite were apparent at the phylum level, with increases (e.g., *Bacteroidetes*, *Spirochaetes*, *Fibrobacteres*, and *Planctomycetes*) and decreases (e.g., *Proteobacteria*, *Cloacimonetes*, and *Hydrogendentes*) in the relative abundance of different phyla. Notably, the abundance of the putative electroactive genus *Paludibacter*[33,34] (OTUs B1 and B3) increased dramatically from less than 10% to nearly 50% between Phases M0 and M8 (Figure 4). Although present in low numbers, electroactive *Geobacter* and *Sphaerochaeta* genera,[35] which were not detected in Phase M0, also exhibited a significant increase in relative abundance under magnetite-added conditions during Phases M8 and M20 (*Geobacter*, 0.3–0.5%;

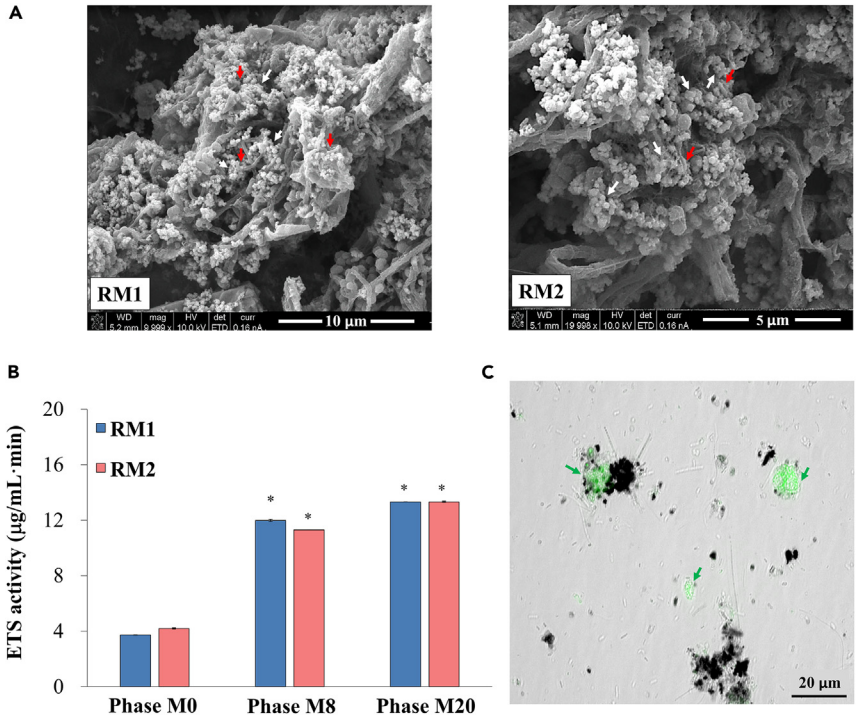

Figure 3. Scanning electron microscopy images of RM1 and RM2 sludge samples collected in Phase M20 (A) ETS activity of reactor sludge at each experimental phase (B), deposition of extracellular S^0 in RM1 sludge (Phase M8) visualized by fluorescence microscopy with a sulfane sulfur-specific probe SSP4 (C)

(A and C) Magnetite particles, cells, and S^0 are indicated by white, red, and green arrows, respectively.

(B) Asterisks indicate statistically significant differences ($p < 0.05$) in ETS activity compared to Phase M0. Error bars present standard deviations of triplicate measurements.

Sphaerochaeta, 0.5–4.2%) (Figure S4A). Interestingly, magnetite addition also significantly affected the community structure of sulfate-reducing bacteria (SRB). The relative abundance of *Desulfomicrobium*, the major SRB genus comprising more than 20% of the total bacteria in Phase M0, decreased sharply to below 2% in the following phases, whereas that of the genus *Desulfobulbus* remained at similar or higher levels in the presence of magnetite (Figures 4 and S4B). These different responses can be explained by the fact that *Desulfobulbus* species possess the *omcF* gene encoding a *c*-type outer membrane cytochrome for extracellular electron transfer and are probably DIET-active in anaerobic sulfate-containing environments,[36] but *Desulfomicrobium* species have not been shown to grow syntrophically.[37] The above results suggest that magnetite enriched diverse electroactive bacteria and promoted electro-syntrophic associations via DIET in the reactor microbial communities.

It is noteworthy that known anaerobic sulfide-oxidizing bacteria (ASOB), such as purple sulfur bacteria, purple non-sulfur bacteria, green sulfur bacteria and nitrate-dependent sulfide-oxidizing bacteria,[38,39] were not detected in any of the reactor samples, although a considerable amount of extracellular S^0 was generated in Phases M8 and M20. The absence of these ASOB is understandable given that the experimental reactors were run anaerobically in the dark with a negligible amount of nitrate (0.0–0.3 mg NO_3^--N/L). It is therefore likely that the sulfide oxidation to S^0 in the presence of magnetite was mediated by unknown ASOB, presumably such as the populations belonging to the phyla *Fibrobacteres* and *Planctomycetes*. The relative abundance of these phyla increased significantly with the addition of magnetite (Figure S4C), as observed in our previous study.[12] *Fibrobacteres* shares a unique common ancestor and is closely related with the phylum *Chlorobi*, which contains green sulfur bacteria (i.e., *Chlorobiaceae*) that phototrophically oxidize sulfide and deposit extracellular S^0 globules.[40,41] These bacteria have flavocytochrome *c*-sulfide dehydrogenate catalyzing H_2S-dependent cytochrome *c* reduction, which enables the sulfide oxidation to S^0 outside the cells.[42] Given that outer membrane *c*-type cytochromes play an important role in extracellular electron transfer in exoelectrogens[24] and many neighboring families of *Chlorobiaceae* are chemoheterotrophic,[43,44] it could be possible that unknown *Fibrobacteres* bacteria

OTU	Classification[a]	Phase M0		Phase M8		Phase M20	
		RM1	RM2	RM1	RM2	RM1	RM2
A1	*Methanothrix* (g)	91.6	90.5	8.4	4.8	4.3	2.1
A2	*Methanothrix* (g)	–[c]	–	75.5	82.4	80.2	84.0
A3	*Methanobacteriaceae* (f)	–	–	0.3	0.5	0.5	0.0
A4	*Methanolinea* (g)	–	–	9.8	7.1	10.8	11.0
A5	*Methanothrix* (g)	4.1	6.3	5.0	4.2	1.4	1.6
A6	*Euryarchaeota* (p)	3.9	2.9	–	–	–	–
A7	*Methanocella* (g)	–	–	0.9	0.6	1.9	0.7
A8	*Pacearchaeota* (p)	0.0	0.1	–	–	–	–
A9	*Methanomassiliicoccus* (g)	–	–	–	–	0.1	0.4
B1	*Paludibacter* (g)	2.6	8.3	49.0	45.0	35.5	21.2
B2	*Bacteroidetes* (p)	0.0	–	7.5	2.4	14.1	3.7
B3	*Paludibacter* (g)	1.6	1.3	0.3	4.6	0.8	28.6
B4	*Desulfomicrobium* (g)	22.2	26.1	2.0	1.3	1.0	0.8
B5	*Bacteroidetes* (p)	0.3	2.8	5.0	6.6	7.5	7.6
B6	*Desulfobulbus* (g)	6.0	2.4	7.5	4.9	5.3	2.7
B7	*Smithella* (g)	3.6	2.7	4.4	4.8	4.6	5.2
B8	*Sulfuricurvum* (g)	3.0	10.6	–	–	0.0	0.0
B9	*Sulfurimonas* (g)	13.8	0.2	–	–	–	–
B10	*Bacteroidetes* (p)	0.0	0.0	2.3	0.4	3.1	0.4
B11	*Bacteroidetes* (p)	1.0	13.2	0.3	0.4	0.3	0.1
B12	*Candidatus* Cloacamonas (g)	0.7	2.0	–	–	–	–
B13	*Sphaerochaeta* (g)	–	–	0.5	2.6	3.6	4.2
B14	*Bacteroidetes* (p)	2.2	0.0	0.5	0.1	1.6	1.2
B15	*Sulfurovum* (g)	6.5	0.0	–	–	–	–
B16	*Syntrophaceae* (f)	0.1	0.1	2.1	1.6	2.7	1.8
B17	*Syntrophaceae* (f)	0.0	0.0	2.3	1.4	1.7	0.7
B18	*Planctomycetaceae* (f)	–	–	1.0	2.1	0.8	1.2
B19	*Bacteroidetes* (p)	3.9	2.3	–	–	–	–
B20	*Parabacteroides* (g)	0.0	2.3	0.3	1.4	0.0	0.2
B21	*Rhodobacter* (g)	0.3	2.1	–	0.0	–	–
B22	*Bacteroides* (g)	–	0.0	0.5	2.3	0.2	1.2
B23	*Cloacimonetes* (p)	2.4	0.2	–	–	–	–
B24	*Deltaproteobacteria* (c)	–	–	0.6	0.2	2.3	0.0

Figure 4. Taxonomic affiliation and relative abundance (%) of major OTUs (>2% in at least one archaeal or bacterial library)
Cells with relative abundance values are colored in a heatmap-like fashion: green for archaeal and red for bacterial sequences. OTU, operational taxonomic unit. [a] The lowest rank assigned by UCLUST against the RDP database (p, phylum; c, class; f, family; g, genus). [b] Not detected at all (zero read). Please note that '0.0' means non-zero read, but in very low relative abundance (<0.1%).

chemotrophically contributed to the oxidation of sulfide to S^0 through DIET-based syntrophy.[12] In support of this suggestion, the growth of green sulfur bacteria in light-limited anaerobic environments, such as deep seawater and hydrothermal vents, has been observed.[41,45,46] *Planctomycetes* species have membrane-bound polysulfide reductase oxidizing sulfide to S^0, which is common in known ASOB, such as

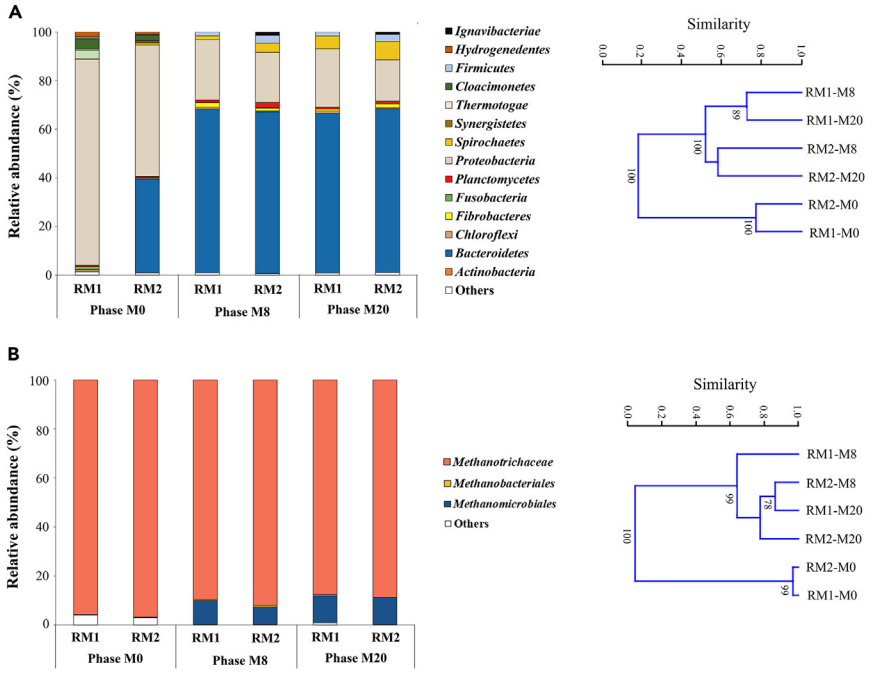

Figure 5. Taxonomic distribution of retrieved sequences and cluster dendrograms constructed from the distribution of OTUs in the bacterial (A) and archaeal (B) 16S rRNA gene libraries of reactor samples

Each sample is labeled with the corresponding reactor name and experimental phase. Sequences with a relative abundance lower than 1% in all samples were classified as 'Others'. Bootstrap values higher than 70% (1,000 replicates) are shown at the nodes in the dendrograms.

Wolinella and *Chlorobium* species.[47,48] *Planctomycetes* cells have unique electron-dense crateriform structures scattered over the cell surface[43] and a comparative genomic study found a putative extracellular electron transfer gene cluster (PCC4) in *Planctomycetes* species.[49] It is therefore possible that unknown *Planctomycetes* bacteria participated in the electric syntrophy for the oxidation of sulfide to S^0.

The methanogenic community was dominated by the family *Methanotrichaceae* (>86% of the total archaea in all 16S rRNA libraries) across the experimental phases (Figure 5B). Of note is the drastic dominance shift between two major *Methanothrix* OTUs (A1 and A2) with the addition of magnetite (Figure 4). OTU A1 was the most abundance methanogenic population, accounting for more than 90% of the total archaeal sequences in Phase M0; however, its relative abundance dropped to 2.1–8.4% in Phases M8 and M20. Conversely, OTU A2, which was not detected in the absence of magnetite, became the most abundant methanogenic population in the presence of magnetite. Meanwhile, correlation analysis based on the relative abundance of OTUs found that OTU A2 correlated positively with the magnetite dose and negatively with the H_2S content in biogas ($p < 0.05$), whereas OTU A1 showed the opposite pattern (Figure S5). Given the recent finding that *Methanothrix*, previously thought to be strictly aceticlastic, can electrotrophically reduce CO_2 to methane.[50] These results suggest that the addition of magnetite stimulated OTU A2, which is possibly more electroactive and less tolerant to sulfate-reducing conditions, over OTU A1. Electro-syntrophic methanogenesis through magnetite-mediated DIET appears to have developed as a major route of methane production in Phases M8 and M20. Furthermore, OTU A2 also had significant positive correlations with the extracellular S^0 concentration and the *Planctomycetaceae*-related OTU B18 ($p < 0.05$). This supports the possibility noted above that unknown *Planctomycetes* bacteria, particularly OTU B18, were involved in the syntrophic oxidation of sulfide to S^0, which was likely coupled to electrotrophic methanogenesis through DIET. Meanwhile, the relative abundance of the hydrogenotrophic order *Methanomicrobiales* represented by OTU A4 increased notably with the addition of magnetite (Figures 4 and 5B), and it had a significant positive correlation with the magnetite dose ($p < 0.05$) (Figure S5). An enrichment of *Methanomicrobiales* in the presence of conductive material has been reported in several studies[51] and a recent study revealed that *Methanospirillum hungatei* belonging to this order has electrically conductive extracellular filaments, although their function has yet to be elucidated.[52] Therefore, although the DIET ability of

Table 2. Production of methane, H_2S, and total dissolved sulfide in semi-continuous bottle cultures with or without magnetite and methanogenic inhibitors

Culture	Magnetite (20 mM Fe)	Inhibitor[a]	CH_4 production rate (mL/d)	CH_4 content in biogas (%)	H_2S production rate (mL/d)	H_2S content in biogas (ppmv)	Total dissolved sulfide (mg/L)
C	–[b]	–	5.1–7.0	10.8–39.6	0.03–0.06	2,196–3,577	61.0–70.3
M	+[c]	–	4.6–7.3	10.5–40.8	0.001–0.003*,#	69–126*,#	59.6–71.0
MB	+	BES	0.03–0.06*,†,‡	0.3–0.4*,†,‡	0.02–0.03†,‡	1,292–3,489†,‡	59.5–66.3
MF	+	Fluoroacetate	3.8–6.5	11.9–14.6	0.001–0.003*,#	50–136*,#	46.1–62.0

Symbols indicate statistically significant differences ($p < 0.05$) compared to C cultures (*), MB cultures (#), M cultures (†), and MF cultures (‡).
[a]BES to inhibit all methanogenic pathways and fluoroacetate to selectively inhibit the aceticlastic pathway.
[b]Not added.
[c]Added.

Methanomicrobiales species has not been verified in defined co-cultures,[53] magnetite may have stimulated the electro-syntrophic growth of *Methanomicrobiales*. It may also be possible that the enrichment of syntrophic VFA-oxidizing *Syntrophaceae* populations (OTUs B7, B16 and B17), possibly capable of both IIET and DIET,[54,55] facilitated the growth of hydrogenotrophic methanogens in Phases M8 and M20. Overall, it appears that magnetite addition created a DIET-promoting environment and enriched different electroactive microorganisms in the experimental reactors.

Electro-syntrophic coupling of sulfide oxidation and electrotrophic methanogenesis

Calculations based on the formal reduction potential ($E^{0\prime}$, vs. standard hydrogen electrode at pH 7°C and 25°C) indicated that, among many reduction reactions commonly occurring in AD processes, the reductions of CO_2 to CH_4 and of SO_4^{2-} to H_2S can be coupled with the oxidation of sulfide to S^0 to form a spontaneous redox process (Reactions 1–4).[56,57]

$$S^0 + H^+ + 2e^- \rightarrow HS^- \; E^{0\prime} = -0.270 \text{ V (Reaction 1)}$$

$$S^0 + 2H^+ + 2e^- \rightarrow H_2S \; E^{0\prime} = -0.274 \text{ V (Reaction 2)}$$

$$SO_4^{2-} + 10H^+ + 8e^- \rightarrow H_2S + 4H_2O \; E^{0\prime} = -0.220 \text{ V (Reaction 3)}$$

$$CO_2 + 8H^+ + 8e^- \rightarrow CH_4 + 2H_2O \; E^{0\prime} = -0.244 \text{ V (Reaction 4)}$$

However, as in our previous study,[12] only the electrotrophic reduction of CO_2 to CH_4 (Reaction 4) was able to make the overall reaction thermodynamically favorable ($E^{0\prime}_{cell}$ = 0.132–0.346 V in Phases M8 and M20) when taking into account the measured concentrations of reactants and products in the reactors. This result suggests that electrotrophic methanogenesis was likely the electron-accepting reaction coupled with the anaerobic oxidation of sulfide to S^0 through DIET.

To verify the formation of the proposed electric syntrophy, semi-continuous cultures (140-mL working volume and 20-day hydraulic retention time [HRT]) inoculated with the sludge taken from RM1 in Phase M20 were incubated with or without the continuous addition of magnetite (20 mM Fe) (Figure 1). During 28 days of incubation, the cultures with (M) or without (C) magnetite addition showed comparable sulfate-reducing activities (i.e., comparable TDS concentrations) and methane productivities (Table 2). Meanwhile, in C cultures, the extracellular S^0 concentration decreased over time (4.8 mg/L on Day 28), along with an accumulation of H_2S (3,577 ppmv in biogas), as the magnetite derived from the RM1 sludge was washed out with the effluent (Figure 6). However, in M cultures, the extracellular S^0 concentration increased with cultivation and reached approximately 60 mg/L, with the H_2S content of the biogas remaining low at 69–126 ppmv. These results agree with the observations in RM1 and RM2 and further confirm the essential role of magnetite in the anaerobic oxidation of sulfide to S^0. Notably, MB cultures supplemented with magnetite and 2-bromoethanesulfonate (BES; 50 mM), a potent inhibitor of all methanogenic pathways,[58] which were tested in parallel with C and M cultures, showed a significantly faster decrease in the extracellular S^0

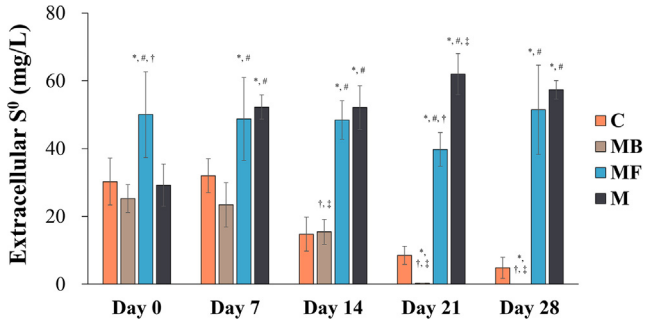

Figure 6. Temporal changes in extracellular S^0 concentrations in semi-continuous bottle cultures with or without magnetite and methanogenic inhibitors: M cultures supplemented with magnetite (20 mM Fe), MB cultures supplemented with magnetite and BES (50 mM), and C cultures with neither magnetite nor BES (control)

After 28 days of cultivation, M cultures were supplemented with fluoroacetate (1 mM) and further incubated for 28 days (referred to as MF cultures). Error bars are standard deviations of quadruplicate cultures. Symbols indicate statistically significant differences ($p < 0.05$) compared to C cultures (*), MB cultures (#), M cultures (†), and MF cultures (‡).

concentration (complete removal in 21 days of incubation) than C cultures. Virtually no methane was produced in MB cultures, with the H_2S content in biogas remaining comparable to that in C cultures. Therefore, it was demonstrated that active methanogenesis is essential for the anaerobic oxidation of sulfide in the presence of magnetite. For a deeper understanding, M cultures were supplemented with fluoroacetate (20 mM), which selectively inhibits aceticlastic methanogenesis,[58] and renamed MF cultures. Interestingly, the extracellular S^0 concentration in MF cultures did not decrease over time and remained at levels comparable to those in M cultures during 28 days of semi-continuous cultivation. MF cultures still produced methane, although the methane content and production rate were lower compared to C and M cultures, while maintaining a low H_2S content in biogas (50–136 ppmv). In addition, sulfate reduction was active in all tested cultures with comparable TDS concentrations, regardless of the presence or absence of magnetite or methanogenesis inhibitors (Table 2). Overall, the above results confirm that CO_2-reducing methanogenesis, not aceticlastic methanogenesis, is the main reduction reaction driving the syntrophic oxidation of sulfide to S^0 in the presence of magnetite.

The 16S rRNA-targeted HTS results of the biomass samples taken from the tested cultures at the end of the experiment revealed that *Methanothrix* and *Methanobacterium* dominated the methanogenic communities in C and M cultures (>91% of the total archaeal reads) (Figure 7). As expected, there were virtually no active methanogens in MB cultures (≤3 archaeal reads out of >13,024 total prokaryotic reads), while several hundreds and thousands of archaeal reads were identified in all other cultures. Complete inhibition of methanogenesis disturbs the interspecies electron transfer required for the anaerobic degradation of VFAs and suppresses the activity of syntrophic VFA oxidizers.[5] Under the imbalanced conditions in MB cultures (≤3,850 mg VFAs as COD/L), fiber-degrading *Anaerosporobacter* occurred as the dominant fermentative bacteria producing VFAs (Figure S6).[59] The methanogenic communities in MF cultures were dominated by hydrogenotrophic methanogens, especially *Methanobacterium*, which is reasonable because acetate is converted to methane by syntrophic acetate oxidation coupled with hydrogenotrophic methanogenesis when aceticlastic methanogenesis is inhibited.[60,61] Correspondingly, the relative abundance of (putative) syntrophic acetate-oxidizing bacteria belonging to the class *Clostridia*[62–65] increased in MF cultures (Figure S6). Recently, a *Methanobacterium* strain capable of growing via DIET with *Geobacter metallireducens* was reported, although all other strains tested so far were not electroactive.[66] This finding suggests the possibility that *Methanobacterium* thrived in electric syntrophy with ASOB or other electroactive bacteria. However, given that its relative abundance was much lower in the cultures without inhibitors, the predominance of *Methanobacterium* in MF cultures was likely due to the inhibition of aceticlastic methanogens rather than the stimulation of its electro-syntrophic growth. An interesting observation is that a notable amount of *Methanothrix* remained in MF cultures, which contrasts with virtually no detection of methanogens in MB cultures (Figure 7). Given that electrotrophic methanogenesis is the only non-aceticlastic pathway known so far for *Methanothrix*,[50] this result strongly suggests the electrotrophic growth of *Methanothrix* in MF cultures.

Noteworthy is that the relative abundance of *Methanothrix* was significantly lower in MF cultures than in C or M cultures, although MF cultures maintained comparable extracellular S^0 levels to M cultures (Figures 6

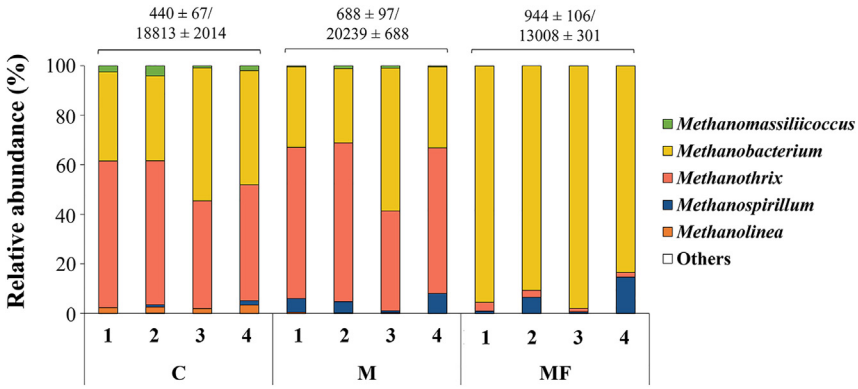

Figure 7. Taxonomic distribution of retrieved archaeal sequences at the genus level in the 16S rRNA gene libraries for semi-continuous cultures with or without magnetite and methanogenic inhibitors: M cultures supplemented with magnetite (20 mM Fe), MB cultures supplemented with magnetite and BES (50 mM), MF cultures supplemented with magnetite and fluoroacetate (1 mM), and C cultures supplemented with none of them (control)

Samples for analysis were taken from each of the quadruplicate bottles at the end of the incubation. The average numbers of prokaryotic and archaeal sequences (average ±standard deviation) from quadruplicates are indicated on top of the bars (prokaryotes/archaea). Sequences with a relative abundance lower than 1% in all samples were classified as 'Others'. MB cultures were excluded from analysis since virtually no archaeal sequences were detected (≤3 out of ≥13,024 prokaryotic sequences).

and 7). This result suggests that electro-syntrophic methanogenesis using sulfide as an electron donor could support substantially less growth of *Methanothrix* in MF cultures compared to its growth in C and M cultures, in which aceticlastic methanogenesis was not inhibited. The limited contribution of electro-syntrophic methanogenesis to the growth of *Methanothrix*, despite the efficient oxidation of sulfide to S^0, under magnetite-added conditions can be attributed to the production of very marginal amounts of H_2S (i.e., limited electron donor availability) compared to methane in the biogas (<0.07%, v/v) (Table 1). Based on the assumption that all electrons generated during sulfide oxidation to S^0 were used for CO_2-reducing methanogenesis (Reactions 2 and 4), the resulting increase in methane production rate can only be estimated to be approximately 3 mL per day, drawing upon the results obtained from Phases M8 and M20 under steady-state conditions.[12] This finding corresponds to the fact that no significant increase in methane production was observed as a consequence of promoted electro-syntrophic methanogenesis in the experimental reactors, although extracellular S^0 accumulated with the addition of magnetite (Figure 2; Table 1).

Electrotrophic Methanothrix as electron acceptor for sulfide oxidation

To verify the contribution of *Methanothrix* to the electro-syntrophic oxidation of sulfide to S^0, a set of DNA stable-isotope probing (SIP) experiments was performed. The quadruplicates of C cultures were divided into two groups of duplicate cultures amended with ^{13}C-bicarbonate, one with magnetite addition (SM) and the other without (SC), and they were cultivated semi-continuously in the same manner as C cultures (Figure 1). In agreement with the observations in C and M cultures, a significant formation of extracellular S^0 was observed only in SM cultures. After three volume turnovers to allow sufficient time for metabolizing ^{13}C-bicarbonate, the 16S rRNA gene concentrations of *Methanothrix* and archaea were analyzed by digital polymeric chain reaction (dPCR) for each culture. *Methanothrix* accounted for the majority of ^{13}C-labeled archaea, with even higher *Methanothrix*-to-archaea ratios than those in the ^{12}C-DNA libraries, in SM cultures, whereas the presence of ^{13}C-labeled *Methanothrix* (and other methanogens) was negligible in SC cultures (Table 3). This result confirms that magnetite promoted the electrotrophic growth of *Methanothrix* given that it is the only route through which *Methanothrix* can utilize CO_2 for methanogenesis.[3] Although acetate generated by homoacetogenesis from H_2 and CO_2 might be aceticlastically utilized by *Methanothrix*,[67] the large difference in the enrichment of ^{13}C-labeled *Methanothrix* between SC and SM cultures shows that its effect is marginal.

The results of the series of experiments discussed above collectively demonstrate that the anaerobic oxidation of sulfide to S^0 can be driven by electrotrophic methanogenesis, especially by *Methanothrix*, via mineral-mediated DIET in sulfur-rich methanogenic environments. This study is the first to demonstrate the occurrence of this type of electric syntrophy, uncovering a new route for anaerobic sulfur metabolism.

Table 3. Concentrations of archaeal and *Methanothrix* 16S rRNA genes in the ^{13}C- and ^{12}C-DNA fractions from DNA-stable isotope probing experiments with ^{13}C-bicarbonate in semi-continuous bottle cultures with or without magnetite

Fraction	C6ulture	Magnetite[a]	16S rRNA gene concentration (copies/g DNA)		*Methanothrix*/archaea ratio (%)
			Archaea	*Methanothrix*	
^{13}C	SC1	–	ND[b]	ND	n.a.[c]
	SC2	–	ND	ND	n.a.
	SM1	+	8.8×10^{12}*	6.0×10^{12}*	68.5%*
	SM2	+	1.4×10^{13}*	1.2×10^{13}*	83.4%*
^{12}C	SC1	–	1.4×10^{13}	8.9×10^{12}	61.8%
	SC2	–	1.5×10^{13}	9.1×10^{12}	59.0%
	SM1	+	7.4×10^{12}	3.8×10^{12}	51.1%
	SM2	+	1.0×10^{13}	6.4×10^{12}	64.6%

Asterisks indicate statistically significant differences ($p < 0.05$) compared to SC cultures.
[a]+, added (20 mM Fe); –, not added.
[b]Not detected. DNA concentration was below the detection limit (<0.010 μg/mL).
[c]Not applicable.

Sulfur is an essential element in all living organisms and is widely distributed in the Earth's crust (approximately 0.05% of the lithosphere's weight).[68] Given the abundance of conductive minerals, such as magnetite and other metal ores, in nature, it is likely that electro-syntrophic sulfide oxidation plays a significant role in the global sulfur cycle and affects the fate of other elements, particularly in anaerobic environments – for example, carbon in methanogenesis. Furthermore, this newly found electric syntrophy presents an interesting possibility for *in situ* H_2S control and S^0 recovery in anaerobic digesters, leading to improved process stability and economy.[12] While substantial further research is required for practical application, the magnetic separation of cell-magnetite aggregates from the effluent may offer a feasible strategy for S^0 recovery and microbial retention.[21] As numerous electro-syntrophic associations exist and respond differently to environmental conditions in anaerobic digesters, understanding the interactions among electroactive microorganisms is important in engineering DIET to enhance digester performance and stability.

Conclusions

A novel electric syntrophy coupling anaerobic sulfide oxidation to S^0 with electrotrophic CO_2 reduction to methane was confirmed by a polyphasic approach including physicochemical, electrochemical, microscopic, and molecular analyses. Magnetite addition induced microbial oxidation of sulfide to S^0 during the AD of sulfur-rich waste mixtures, significantly decreasing the H_2S production in biogas. The enrichment of diverse electroactive microorganisms and the increase in ETS activity under magnetite-supplemented conditions suggested the involvement of DIET. Experiments on semi-continuous cultures with methanogenic inhibitors (BES and fluoroacetate) and ^{13}C-bicarbonate (DNA-SIP) revealed that the anaerobic oxidation of sulfide to S^0 was coupled by DIET with electrotrophic methanogenesis, especially by *Methanothrix*. This study is the first to confirm a novel electric syntrophy coupling the oxidation of sulfide to S^0 with the electrotrophic reduction of CO_2 to methane in anaerobic environments. Although more research is needed to identify the exoelectrogenic ASOB in syntrophy with electrotrophic methanogens and to better understand their interactions, this newly discovered syntropy likely contributes to the cycling of sulfur in both natural and engineered anaerobic environments.

Limitations of the study

While we demonstrated in this study the occurrence of a novel electric syntrophy, coupling anaerobic sulfide oxidation to S^0 with electrotrophic CO_2 reduction to CH_4, using a polyphasic approach, we were unable to directly observe the flow of electrons from the former to the latter reactions due to technological limitations. Although *Methanothrix* was identified as the major electrotrophic methanogen involved in this syntrophy, the possibility of other microorganisms directly accepting electrons from the sulfide oxidation cannot be ruled out due to the complex nature of methanogenic microbial communities. We did not identify the

exoelectrogenic ASOB in syntrophy with *Methanothrix*, despite proposing *Fibrobacteres*-and *Planctomycetes*-related bacteria as potential candidates. These outstanding questions merit further research for a deeper understanding of the electro-syntrophic interactions in anaerobic microbial communities.

STAR★METHODS

Detailed methods are provided in the online version of this paper and include the following:

- KEY RESOURCES TABLE
- RESOURCE AVAILABILITY
  - Lead contact
  - Materials availability
  - Data and code availability
- EXPERIMENTAL MODEL AND SUBJECT DETAILS
- METHOD DETAILS
  - Reactor setup and operation
  - Batch and semi-continuous culture tests
  - Extracellular elemental sulfur analysis
  - Electron transport system activity
  - Cyclic voltammetry
  - Scanning electron microscopy
  - Microbial community analysis
  - DNA stable-isotope probing and digital PCR
  - Other analytical methods
- QUANTIFICATION AND STATISTICAL ANALYSIS

SUPPLEMENTAL INFORMATION

Supplemental information can be found online at https://doi.org/10.1016/j.isci.2023.107504.

ACKNOWLEDGMENTS

This research was supported by grants from the National Research Foundation of Korea funded by the Korea Ministry of Science and ICT (2020R1A2C2004368 and 2020K1A4A7A02108858).

AUTHOR CONTRIBUTIONS

Conceptualization, H.J. and C.L.; Validation, H.J.; Visualization, H.J.; Formal analysis, H.J. and H.Y.; Writing–original draft; H.J., Writing–review and editing, H.J., H.Y., and C.L.; Funding acquisition and Supervision, C.L.

DECLARATION OF INTERESTS

The authors declare that they have no known competing financial interests or personal relationships that could have appeared to influence the work reported in this paper.

Received: February 28, 2023
Revised: April 3, 2023
Accepted: July 26, 2023
Published: August 1, 2023

REFERENCES

1. Morita, M., Malvankar, N.S., Franks, A.E., Summers, Z.M., Giloteaux, L., Rotaru, A.E., Rotaru, C., and Lovley, D.R. (2011). Potential for direct interspecies electron transfer in methanogenic wastewater digester aggregates. mBio *2*, e00159-11. https://doi.org/10.1128/mBio.00159-11.

2. Kato, S., Hashimoto, K., and Watanabe, K. (2012). Methanogenesis facilitated by electric syntrophy via (semi)conductive iron-oxide minerals. Environ. Microbiol. *14*, 1646–1654. https://doi.org/10.1111/j.1462-2920.2011.02611.x.

3. Rotaru, A.E., Shrestha, P.M., Liu, F., Markovaite, B., Chen, S., Nevin, K.P., and Lovley, D.R. (2014). Direct interspecies electron transfer between *Geobacter metallireducens* and *Methanosarcina barkeri*. Appl. Environ. Microbiol. *80*, 4599–4605. https://doi.org/10.1128/AEM.00895-14.

4. Lovley, D.R. (2011). Live wires: direct extracellular electron exchange for bioenergy and the bioremediation of energy-related contamination. Energy Environ. Sci. *4*, 4896–4906. https://doi.org/10.1039/C1EE02229F.

5. Baek, G., Kim, J., Kim, J., and Lee, C. (2018). Role and potential of direct interspecies electron transfer in anaerobic digestion. Energies *11*, 107. https://doi.org/10.3390/en11010107.

6. Barua, S., and Dhar, B.R. (2017). Advances towards understanding and engineering direct interspecies electron transfer in anaerobic digestion. Bioresour. Technol. *244*, 698–707. https://doi.org/10.1016/j.biortech.2017.08.023.

7. Zhao, Z., Li, Y., Zhang, Y., and Lovley, D.R. (2020). Sparking anaerobic digestion: promoting direct interspecies electron transfer to enhance methane production. iScience *23*, 101794. https://doi.org/10.1016/j.isci.2020.101794.

8. Shrestha, P.M., and Rotaru, A.E. (2014). Plugging in or going wireless: Strategies for interspecies electron transfer. Front. Microbiol. *5*, 237. https://doi.org/10.3389/fmicb.2014.00237.

9. Van Steendam, C., Smets, I., Skerlos, S., and Raskin, L. (2019). Improving anaerobic digestion via direct interspecies electron transfer requires development of suitable characterization methods. Curr. Opin. Biotechnol. *57*, 183–190. https://doi.org/10.1016/j.copbio.2019.03.018.

10. Lovley, D.R. (2017). Syntrophy Goes electric: Direct interspecies electron transfer. Annu. Rev. Microbiol. *71*, 643–664. https://doi.org/10.1146/annurev-micro-030117-020420.

11. Logan, B.E., Rossi, R., Ragab, A., and Saikaly, P.E. (2019). Electroactive microorganisms in bioelectrochemical systems. Nat. Rev. Microbiol. *17*, 307–319. https://doi.org/10.1038/s41579-019-0173-x.

12. Jung, H., Baek, G., and Lee, C. (2020). Magnetite-assisted *in situ* microbial oxidation of H_2S to S^0 during anaerobic digestion: A new potential for sulfide control. Chem. Eng. J. *397*, 124982. https://doi.org/10.1016/j.cej.2020.124982.

13. Wellinger, A., and Lindberg, A. (2001). Biogas Upgrading and Utilisation-IEA Bioenergy, Task 24-Energy from Biological Conversion of Organic Waste.

14. Jung, H., Kim, J., and Lee, C. (2019). Temperature effects on methanogenesis and sulfidogenesis during anaerobic digestion of sulfur-rich macroalgal biomass in sequencing batch reactors. Microorganisms *7*, 682. https://doi.org/10.3390/microorganisms7120682.

15. Muñoz, R., Meier, L., Diaz, I., and Jeison, D. (2015). A review on the state-of-the-art of physical/chemical and biological technologies for biogas upgrading. Rev. Environ. Sci. Biotechnol. *14*, 727–759. https://doi.org/10.1007/s11157-015-9379-1.

16. Jiao, P., Zhang, X., Qiu, S., Zhou, X., Tian, Z., Liang, Y., Zhang, Y., and Ma, L. (2023). Pyrite-enhanced sludge digestion via stimulation of direct interspecies electron transfer between syntrophic propionate- and sulfur-oxidizing bacteria and methanognes: Genome-centric metagenomic evidence. Chem. Eng. J. *456*, 141089. https://doi.org/10.1016/j.cej.2022.141089.

17. Jung, H., Kim, D., Choi, H., and Lee, C. (2022). A review of technologies for in-situ sulfide control in anaerobic digestion. Renew. Sustain. Energy *157*, 112068. https://doi.org/10.1016/j.rser.2021.112068.

18. Lin, H.S., Peel, N.M., Hubbard, R.E., and Hu, B. (2016). Electrochemical sulfide removal by low-cost electrode materials in anaerobic digestion. Chem. Eng. J. *5*, 180–182. https://doi.org/10.1016/j.cej.2016.03.086.

19. Whiteman, M., and Moore, P.K. (2009). Hydrogen sulfide and the vasculature: a novel vasculoprotective entity and regulator of nitric oxide bioavailability? J. Cell Mol. Med. *13*, 488–507. https://doi.org/10.1111/j.1582-4934.2009.00645.x.

20. Poulton, S.W., Krom, M.D., and Raiswell, R. (2004). A revised scheme for the reactivity of iron (oxyhydr) oxide minerals towards dissolved sulfide. Geochim. Cosmochim. Acta *68*, 3703–3715. https://doi.org/10.1016/j.gca.2004.03.012.

21. Baek, G., Jung, H., Kim, J., and Lee, C. (2017). A long-term study on the effect of magnetite supplementation in continuous anaerobic digestion of dairy effluent–magnetic separation and recycling of magnetite. Bioresour. Technol. *241*, 830–840. https://doi.org/10.1016/j.biortech.2017.06.018.

22. Baek, G., Kim, J., Kim, J., and Lee, C. (2020). Individual and combined effects of magnetite addition and external voltage application on anaerobic digestion of dairy wastewater. Bioresour. Technol. *297*, 122443. https://doi.org/10.1016/j.biortech.2019.122443.

23. de Bok, F.A.M., Plugge, C.M., and Stams, A.J.M. (2004). Interspecies electron transfer in methanogenic propionate degrading consortia. Water Res. *38*, 1368–1375. https://doi.org/10.1016/j.watres.2003.11.028.

24. Lovley, D.R. (2017). Happy together: microbial communities that hook up to swap electrons. ISME J. *11*, 327–336. https://doi.org/10.1038/ismej.2016.136.

25. Chen, S., Rotaru, A.E., Liu, F., Philips, J., Woodard, T.L., Nevin, K.P., and Lovley, D.R. (2014). Carbon cloth stimulates direct interspecies electron transfer in syntrophic co-cultures. Bioresour. Technol. *173*, 82–86. https://doi.org/10.1016/j.biortech.2014.09.009.

26. Liu, F., Rotaru, A.E., Shrestha, P.M., Malvankar, N.S., Nevin, K.P., and Lovley, D.R. (2012). Promoting direct interspecies electron transfer with activated carbon. Energy Environ. Sci. *5*, 8982–8989. https://doi.org/10.1039/C2EE22459C.

27. Jiang, Q., Wu, P., Zhang, X., Zhang, Y., Cui, M., Liu, H., and Liu, H. (2022). Deciphering the effects of engineered biochar on methane production and the mechanisms during anaerobic digestion: Surface functional groups and electron exchange capacity. Energy Convers. Manag. *258*, 115417. https://doi.org/10.1016/j.enconman.2022.115417.

28. Yin, Q., He, K., Liu, A., and Wu, G. (2017). Enhanced system performance by dosing ferroferric oxide during the anaerobic treatment of tryptone-based high-strength wastewater. Appl. Microbiol. Biotechnol. *101*, 3929–3939. https://doi.org/10.1007/s00253-017-8194-8.

29. Chen, S., Tao, Z., Yao, F., Wu, B., He, L., Hou, K., Pi, Z., Fu, J., Yin, H., Huang, Q., et al. (2020). Enhanced anaerobic co-digestion of waste activated sludge and food waste by sulfidated microscale zerovalent iron: Insights in direct interspecies electron transfer mechanism. Bioresour. Technol. *316*, 123901. https://doi.org/10.1016/j.biortech.2020.123901.

30. Li, Y., Tang, Y., Xiong, P., Zhang, M., Deng, Q., Liang, D., Zhao, Z., Feng, Y., and Zhang, Y. (2020). High-efficiency methanogenesis via kitchen wastes served as ethanol source to establish direct interspecies electron transfer during anaerobic co-digestion with waste activated sludge. Water Res. *176*, 115763. https://doi.org/10.1016/j.watres.2020.115763.

31. Yin, Q., Yang, S., Wang, Z., Xing, L., and Wu, G. (2018). Clarifying electron transfer and metagenomic analysis of microbial community in the methane production process with the addition of ferroferric oxide. Chem. Eng. J. *333*, 216–225. https://doi.org/10.1016/j.cej.2017.09.160.

32. Zhuang, H., Zhu, H., Shan, S., Zhang, L., Fang, C., and Shi, Y. (2018). Potential enhancement of direct interspecies electron transfer for anaerobic degradation of coal gasification wastewater using up-flow anaerobic sludge blanket (UASB) with nitrogen doped sewage sludge carbon assisted. Bioresour. Technol. *270*, 230–235. https://doi.org/10.1016/j.biortech.2016.03.005.

33. Wang, Z., Yin, Q., Gu, M., He, K., and Wu, G. (2018). Enhanced azo dye Reactive Red 2 degradation in anaerobic reactors by dosing conductive material of ferroferric oxide. J. Hazard Mater. *357*, 226–234. https://doi.org/10.1016/j.jhazmat.2018.06.005.

34. Zakaria, B.S., Lin, L., and Dhar, B.R. (2019). Shift of biofilm and suspended bacterial communities with changes in anode potential in a microbial electrolysis cell treating primary sludge. Sci. Total Environ. *689*, 691–699. https://doi.org/10.1016/j.scitotenv.2019.06.519.

35. Zhao, Z., Wang, J., Li, Y., Zhu, T., Yu, Q., Wang, T., Liang, S., and Zhang, Y. (2020). Why do DIETers like drinking: Metagenomic analysis for methane and energy metabolism during anaerobic digestion with ethanol. Water Res. *171*, 115425. https://doi.org/10.1016/j.watres.2019.115425.

36. Zeng, D., Yin, Q., Du, Q., and Wu, G. (2019). System performance and microbial community in ethanol-fed anaerobic reactors acclimated with different organic carbon to sulfate ratios. Bioresour. Technol. *278*, 34–42. https://doi.org/10.1016/j.biortech.2019.01.047.

37. Zhang, Y., Li, J., Liu, F., Yan, H., Li, J., and Zhang, X. (2018). Reduction of Gibbs free energy and enhancement of *Methanosaeta* by bicarbonate to promote anaerobic syntrophic butyrate oxidation. Bioresour. Technol. *267*, 209–217. https://doi.org/10.1016/j.biortech.2018.06.098.

38. Frigaard, N.U. (2016). Biotechnology of Anoxygenic Phototrophic Bacteria. In Anaerobes in Biotechnology, R. Hatti-Kaul, G. Mamo, and B. Mattiasson, eds. (Springer International Publishing), pp. 139–154. https://doi.org/10.1007/10_2015_5006.

39. Shao, M.F., Zhang, T., and Fang, H.H.P. (2010). Sulfur-driven autotrophic denitrification: diversity, biochemistry, and engineering applications. Appl. Microbiol. Biotechnol. *88*, 1027–1042. https://doi.org/10.1007/s00253-010-2847-1.

40. Gupta, R.S. (2004). The phylogeny and signature sequences characteristics of *Fibrobacteres, Chlorobi*, and *Bacteroidetes*. Crit. Rev. Microbiol. *30*, 123–143. https://doi.org/10.1080/10408410490435133.

41. Imhoff, J.F. (2014). The Family Chlorobiaceae (Springer). https://doi.org/10.1007/978-3-642-38954-2_142.

42. Sakurai, H., Ogawa, T., Shiga, M., and Inoue, K. (2010). Inorganic sulfur oxidizing system in green sulfur bacteria. Photosynth. Res. *104*, 163–176. https://doi.org/10.1007/s11120-010-9531-2.

43. Kreig, N.R., Wolfgang, L., William, W., Brain, P.H., Bruce, J.P., James, T.S., Naomi, W., Daniel, B., and Aidan, P. (2011). Volume Four: The *Bacteroidetes, Spirochates, Tenericutes (Mollicutes), Acidobacteria, Fibrobacteres, Fusobacteria, Dictyoglomi, Gemmatimonadetes, Lentisphaerae, Verrucomicrobia, Chlamydiae*, and *Planctomycetes*. Bergey's Manual of Systematic Bacteriology (Springer).

44. Liu, Z., Frigaard, N.U., Vogl, K., Iino, T., Ohkuma, M., Overmann, J., and Bryant, D.A. (2012). Complete genome of *Ignavibacterium album*, a metabolically versatile, flagellated, facultative anaerobe from the phylum *Chlorobi*. Front. Microbiol. *3*, 185. https://doi.org/10.3389/fmicb.2012.00185.

45. Beatty, J.T., Overmann, J., Lince, M.T., Manske, A.K., Lang, A.S., Blankenship, R.E., Van Dover, C.L., Martinson, T.A., and Plumley, F.G. (2005). An obligately photosynthetic bacterial anaerobe from a deep-sea hydrothermal vent. Proc. Natl. Acad. Sci. USA *102*, 9306–9310. https://doi.org/10.1073/pnas.0503674102.

46. Marschall, E., Jogler, M., Henßge, U., and Overmann, J. (2010). Large-scale distribution and activity patterns of an extremely low-light-adapted population of green sulfur bacteria in the Black Sea. Environ. Microbiol. *12*, 1348–1362. https://doi.org/10.1111/j.1462-2920.2010.02178.x.

47. Frigaard, N.U., and Bryant, D.A. (2008). Genomic Insights into the Sulfur Metabolism of Phototrophic Green Sulfur Bacteria. In Sulfur Metabolism in Phototrophic Organisms, R. Hell, C. Dahl, D. Knaff, and T. Leustek, eds. (Springer Netherlands), pp. 337–355. https://doi.org/10.1007/978-1-4020-6863-8_17.

48. Krafft, T., Gross, R., and Kröger, A. (1995). The function of *Wolinella succinogenes* psr genes in electron transport with polysulphide as the terminal electron acceptor. Eur. J. Biochem. *230*, 601–606. https://doi.org/10.1111/j.1432-1033.1995.0601h.x.

49. He, S., Barco, R.A., Emerson, D., and Roden, E.E. (2017). Comparative genomic analysis of neutrophilic iron(ii) oxidizer genomes for candidate genes in extracellular electron transfer. Front. Microbiol. *8*, 1584. https://doi.org/10.3389/fmicb.2017.01584.

50. Rotaru, A.E., Shrestha, P.M., Liu, F., Shrestha, M., Shrestha, D., Embree, M., Zengler, K., Wardman, C., Nevin, K.P., and Lovley, D.R. (2014). A new model for electron flow during anaerobic digestion: direct interspecies electron transfer to *Methanosaeta* for the reduction of carbon dioxide to methane. Energy Environ. Sci. *7*, 408–415. https://doi.org/10.1039/C3EE42189A.

51. Lee, J.Y., Lee, S.H., and Park, H.D. (2016). Enrichment of specific electro-active microorganisms and enhancement of methane production by adding granular activated carbon in anaerobic reactors. Bioresour. Technol. *205*, 205–212. https://doi.org/10.1016/j.biortech.2016.01.054.

52. Walker, D.J.F., Martz, E., Holmes, D.E., Zhou, Z., Nonnenmann, S.S., Lovley, D.R., Papoutsakis, E.T., Courchesne, N.M.D., and Poweleit, N. (2019). The archaellum of *Methanospirillum hungatei* is electrically conductive. mBio *10*, e00579-19. https://doi.org/10.1128/mBio.00579-19.

53. Yee, M.O., and Rotaru, A.-E. (2020). Extracellular electron uptake in *Methanosarcinales* is independent of multiheme c-type cytochromes. Sci. Rep. *10*, 372. https://doi.org/10.1038/s41598-019-57206-z.

54. Baek, G., Kim, J., and Lee, C. (2021). Effectiveness of electromagnetic *in situ* magnetite capture in anaerobic sequencing batch treatment of dairy effluent under electro-syntrophic conditions. Renew. Energy *179*, 105–115. https://doi.org/10.1016/j.renene.2021.07.052.

55. Wang, C., Wang, C., Liu, J., Han, Z., Xu, Q., Xu, X., and Zhu, L. (2020). Role of magnetite in methanogenic degradation of different substances. Bioresour. Technol. *314*, 123720. https://doi.org/10.1016/j.biortech.2020.123720.

56. Aghababaie, M., Farhadian, M., Jeihanipour, A., and Biria, D. (2015). Effective factors on the performance of microbial fuel cells in wastewater treatment–a review. Environ. Technol. Rev. *4*, 71–89. https://doi.org/10.1080/09593330.2015.1077896.

57. Thauer, R.K., Jungermann, K., and Decker, K. (1977). Energy conservation in chemotrophic anaerobic bacteria. Bacteriol. Rev. *41*, 100–180. https://doi.org/10.1128/br.41.3.809-809.1977.

58. Liu, H., Wang, J., Wang, A., and Chen, J. (2011). Chemical inhibitors of methanogenesis and putative applications. Appl. Microbiol. Biotechnol. *89*, 1333–1340. https://doi.org/10.1007/s00253-010-3066-5.

59. Jeong, H., Lim, Y.W., Yi, H., Sekiguchi, Y., Kamagata, Y., and Chun, J. (2007). *Anaerosporobacter mobilis* gen. nov., sp. nov., isolated from forest soil. Int. J. Syst. Evol. Microbiol. *57*, 1784–1787. https://doi.org/10.1099/ijs.0.63283-0.

60. Pan, X., Zhao, L., Li, C., Angelidaki, I., Lv, N., Ning, J., Cai, G., and Zhu, G. (2021). Deep insights into the network of acetate metabolism in anaerobic digestion: focusing on syntrophic acetate oxidation and homoacetogenesis. Water Res. *190*, 116774. https://doi.org/10.1016/j.watres.2020.116774.

61. Werner, J.J., Garcia, M.L., Perkins, S.D., Yarasheski, K.E., Smith, S.R., Muegge, B.D., Stadermann, F.J., DeRito, C.M., Floss, C., Madsen, E.L., et al. (2014). Microbial community dynamics and stability during an ammonia-induced shift to syntrophic acetate oxidation. Appl. Environ. Microbiol. *80*, 3375–3383. https://doi.org/10.1128/AEM.00166-14.

62. Lee, M.J., and Zinder, S.H. (1988). Carbon monoxide pathway enzyme activities in a thermophilic anaerobic bacterium grown acetogenically and in a syntrophic acetate-oxidizing coculture. Arch. Microbiol. *150*, 513–518. https://doi.org/10.1007/BF00408241.

63. Drake, H.L., Küsel, K., and Matthies, C. (2006). Acetogenic prokaryotes. Prokaryotes *2*, 354–420. https://doi.org/10.1007/0387-30742-7_13.

64. Wang, J., Zhong, C., Zhang, X., Liu, H., Ma, D., and Yue, Z. (2020). Quantitative analysis of acetate oxidation in the presence of iron in a thermophilic methanogenic reactor. Renew. Energy *149*, 928–932. https://doi.org/10.1016/j.renene.2019.10.071.

65. Charalambous, P., Shin, J., Shin, S.G., and Vyrides, I. (2020). Anaerobic digestion of industrial dairy wastewater and cheese whey: Performance of internal circulation bioreactor and laboratory batch test at pH 5-6. Renew. Energy *147*, 1–10. https://doi.org/10.1016/j.renene.2019.08.091.

66. Zheng, S., Liu, F., Wang, B., Zhang, Y., and Lovley, D.R. (2020). *Methanobacterium* capable of direct interspecies electron transfer. Environ. Sci. Technol. *54*, 15347–15354. https://doi.org/10.1021/acs.est.0c05525.

67. Liu, R., Hao, X., and Wei, J. (2016). Function of homoacetogenesis on the heterotrophic methane production with exogenous H_2/CO_2 involved. Chem. Eng. J. *284*, 1196–1203. https://doi.org/10.1016/j.cej.2015.09.081.

68. Steudel, R., and amd Eckert, B. (2003). Solid sulfur allotropes. In Elemental Sulfur and Sulfur-Rich Compounds, pp. 1–80. https://doi.org/10.1007/b12110.

69. Jung, H., Kim, J., and Lee, C. (2016). Continuous anaerobic co-digestion of *Ulva* biomass and cheese whey at varying substrate mixing ratios: Different responses in two reactors with different operating regimes. Bioresour. Technol. *221*, 366–374. https://doi.org/10.1016/j.biortech.2016.09.059.

70. Rajeshwari, K.V., Balakrishnan, M., Kansal, A., Lata, K., and Kishore, V.V.N. (2000). State-of-the-art of anaerobic digestion technology for industrial wastewater treatment. Renew. Sustain. Energy Rev. *4*, 135–156. https://doi.org/10.1016/S1364-0321(99)00014-3.

71. Visser, A., Beeksma, I., Van der Zee, F., Stams, A.J.M., and Lettinga, G. (1993). Anaerobic degradation of volatile fatty acids at different sulphate concentrations. Appl. Microbiol. Biotechnol. *40*, 549–556. https://doi.org/10.1007/BF00175747.

72. Zehnder, A.J., Huser, B.A., Brock, T.D., and Wuhrmann, K. (1980). Characterization of an acetate-decarboxylating, non-hydrogen-oxidizing methane bacterium. Arch. Microbiol. *124*, 1–11. https://doi.org/10.1007/BF00407022.

73. Edgar, R.C. (2010). Search and clustering orders of magnitude faster than BLAST. Bioinformatics *26*, 2460–2461. https://doi.org/10.1093/bioinformatics/btq461.

74. Caporaso, J.G., Kuczynski, J., Stombaugh, J., Bittinger, K., Bushman, F.D., Costello, E.K., Fierer, N., Peña, A.G., Goodrich, J.K., Gordon, J.I., et al. (2010). QIIME allows analysis of high-throughput community sequencing data. Nat. Methods *7*, 335–336. https://doi.org/10.1038/nmeth.f.303.

75. Martineau, C., Whyte, L.G., and Greer, C.W. (2008). Development of a SYBR safe™ technique for the sensitive detection of DNA in cesium chloride density gradients for stable isotope probing assays. J. Microbiol. Methods *73*, 199–202. https://doi.org/10.1016/j.mimet.2008.01.016.

76. Jung, H., Kim, J., and Lee, C. (2017). Effect of enhanced biomass retention by sequencing batch operation on biomethanation of sulfur-rich macroalgal biomass: Process performance and microbial ecology. Algal Res. *28*, 128–138. https://doi.org/10.1016/j.algal.2017.10.018.

77. APHA-AWWA_WEF (2005). Standard Methods for the Examination of Water and Wastewater, 21st ed. (American Public Health Association).

78. Thamdrup, B., Fossing, H., and Jørgensen, B.B. (1994). Manganese, iron and sulfur cycling in a coastal marine sediment, Aarhus Bay, Denmark. Geochim. Cosmochim. Acta *58*, 5115–5129. https://doi.org/10.1016/0016-7037(94)90298-4.

STAR★METHODS

KEY RESOURCES TABLE

REAGENT or RESOURCE	SOURCE	IDENTIFIER
Other		
Anaerobic sludge	Full scale AD plant co-digesting sewage sludge and food waste	N/A
Seaweed (*Ulva* sp.)	Naturally produced (Imrang beach, Korea)	N/A
Cheese whey	Dairy processing company (Samik Dairy & Food Co., Korea)	N/A
Chemicals, peptides, and recombinant proteins		
Magnetite (Fe3O4)	JUNSEI, Japan	34380-1501
SSP4	Dojindo, Japan	
Deposited data		
16s rRNA dataset for archaeal and bacterial communities	NCBI Sequence Read Archive	NCBI: PRJNA666182
Oligonucleotides		
Primers for HTS analysis: 515F(ACTCCTACGGGAGGCAG) and 805R(GACTACCAGGGTATCTAATCC)	This study	N/A
Primers for Methanothrix: Mst702F(TAATCCTYGARGGACCACCA) and Mst862R(CCTACGGCACCRACMAC)	This study	N/A
Primers for archaea: ARC787F(ATTAGATACCCSBGTAGTCC) and ARC1059R(GCCATGCACCWCCTCT)	This study	N/A
Software and algorithms		
Cytoscape (ver 3.8.1)	https://cytoscape.org/	N/A
CD-HIT-OTU	http://weizhongli-lab.org/cd-hit-otu/	N/A
UCLUST in the QIIME suite (ver 1.8.0)	Morita et al.[1], Kato et al.[2]	N/A
PAST (ver. 4.03)	https://www.nhm.uio.no/english/research/infrastructure/past/	N/A

RESOURCE AVAILABILITY

Lead contact

Further information and requests for resources should be directed to and will be fulfilled by the lead contact, Changsoo Lee (cslee@unist.ac.kr).

Materials availability

The sequence data generated in this study have been deposited in the NCBI Sequence Read Archive under BioProject accession number PRJNA666182.

Data and code availability

- The published article includes all datasets generated or analyzed during this study.

- Any additional information required to reanalyze the data reported in this paper is available from the lead contact upon request.
- This paper does not report original code.

EXPERIMENTAL MODEL AND SUBJECT DETAILS

This study did not include the experimental models (animals, human subjects, plants, cell lines, primary cell cultures, and computational models).

METHOD DETAILS

Reactor setup and operation

Anaerobic sludge taken from a full-scale AD plant co-digesting sewage sludge and food waste was used as the inoculum for the experimental reactors treating mixtures of green macroalgal *Ulva* biomass and cheese whey. *Ulva* biomass, a major contributor to green tides worldwide, was used as the primary substrate due to its high organic and sulfur contents,[69,70] providing a suitable environment for exploring the fate and effect of sulfur under DIET-promoting conditions. Cheese whey was added to the mixture to adjust the nutrient balance and help stable methanogenesis.[69] Fresh *Ulva* was collected from a local beach, rinsed with a small amount of tap water, and ground into a slurry using a kitchen blender. Whey was obtained from a dairy processing company (Samik Dairy & Food Co., Korea). The *Ulva* slurry and whey were mixed at a COD ratio of 3:1 to prepare the feed mixture with a COD concentration of 5.0 g/L with reference to a previous study of their anaerobic co-digestion at different mixing ratios.[69] The physicochemical characteristics of the inoculum and substrates are presented in Table S1.

RM1 and RM2 with a working volume of 2 L were operated for 545 days. The reactors were fully filled with the inoculum and fed once daily with the feed mixture at a fixed HRT of 20 days. The operating temperature and pH were controlled at 35 $\pm$ 2°C and 7.0 $\pm$ 0.1 (with 3 N of NaOH solution), respectively. Conductive magnetite (100–700-nm particle size) was continuously added to the reactors with the feed at increasing concentrations from 0 to 8 and 20 mM Fe (Phases M0, M8 and M20, respectively). The magnetite dosages were selected based on our previous research, which demonstrated that the H_2S content in biogas decreased significantly with the addition of magnetite.[12] Steady-state data at each experimental phase were collected after at least three turnovers of the working volume.

Batch and semi-continuous culture tests

A set of batch cultures to determine whether the formation of S^0 in the experimental reactors in the presence of magnetite was biological or chemical were performed in 160-mL serum bottles with a working volume of 100 mL. The cultures were divided into one biotic and two abiotic subsets, each of which was tested with and without 20 mM Fe of magnetite (Table S2). The biotic cultures were inoculated with the same inoculum sludge as that used for RM1 and RM2 (50%, v/v), and the abiotic cultures were inoculated with either the inoculum sludge sterilized by autoclaving (121°C, 30 min) or distilled water (50%, v/v). The remaining volume was filled with a modified anaerobic growth medium without sulfate as previously described:[71] $NaHCO_3$, 2000 mg/L; $NaH_2PO_4 \cdot 2H_2O$, 795 mg/L; K_2HPO_4, 600 mg/L; NH_4Cl, 280 mg/L; $CaCl_2 \cdot 7H_2O$, 10 mg/L; yeast extract, 20 mg/L; and trace element solution,[72] 1 mL/L. The cultures were incubated with sodium acetate (5 g COD/L) as the carbon source and either sodium sulfate or sodium sulfide (34 mM S) as the sulfur source. The 12 resulting combinations were tested in quintuplicate.

A set of semi-continuous cultures to confirm whether the anaerobic sulfide oxidation to S^0 was syntrophically coupled to electrotrophic methanogenesis in the presence of magnetite were performed in 250-mL serum bottles with a working volume of 140 mL. The cultures were split into three subsets of quadruplicate cultures: M cultures supplemented with magnetite (20 mM Fe), MB cultures supplemented with magnetite and BES (50 mM), and C cultures supplemented with neither magnetite nor BES (control) (Table S2). Each culture was initially filled with the RM1 mixed liquor collected during Days 496–517 and was fed daily at a 20-day HRT with the feed mixture used for the reactor experiment. After 28 days of cultivation, M cultures were supplemented with fluoroacetate (1 mM) and further incubated for 28 days (referred to as MF cultures) (Table S2).

All batch and semi-continuous cultures were incubated on an orbital shaker (150 rpm) in an anaerobic chamber (Coy Laboratory Products, USA) under an atmosphere of 90% N_2, 5% H_2 and 5% CO_2 (v/v) at

37 ± 1°C. The cultures were purged with the same gas mixture to ensure anaerobic cultivation conditions at the beginning of the experiments.

Extracellular elemental sulfur analysis

A mixed liquor sample for measuring extracellular S^0 was divided into two 20-mL aliquots in 50-mL centrifuge tubes. One aliquot was pelleted by gentle centrifugation and directly used for extracting total cell-associated S^0, while the other, which was used for analyzing intracellular S^0, was pelleted by ultracentrifugation after being treated by a combination of repeated centrifugal washing and ultrasonication, as previously described.[12] The resulting pellets were loosened by vortexing and subjected to S^0 extraction with 20 mL of perchloroethylene in an orbital shaker (280 rpm) for 16 h. The extracts were filtered through a 0.22-μm pore filter and analyzed for S^0 concentration using a 1200 series high-performance liquid chromatograph (Agilent, Germany) installed with a diode array detector and an Acclaim 120 C18 column (Dionex, USA). The concentration of extracellular S^0 was determined as the difference between the concentrations of intracellular S^0 and total cell-associated S^0.[12]

Fluorescence microscopy to visualize extracellular S^0 in the sludge matrix was performed using an SSP4 probe (Dojindo, Japan) specific to sulfane sulfur. A 10-μM SSP4 working solution was prepared in a modified serum-free medium (without cetrimonium bromide, which introduces the SSP4 probe into cells) following the manufacturer's instructions. A 1-mL mixed liquor sample was collected in a 2-mL microcentrifuge tube and washed three times with distilled water by centrifugation (5,000 *g* for 5 min). The resulting pellet was resuspended in 1 mL of the modified serum-free medium, mixed with 1 mL of the SSP4 working solution, and incubated at 37°C for 15 min. The incubated mixture was washed three times with 1 mL of the modified serum-free medium by centrifugation (5,000 *g* for 5 min), and the final resuspension was observed using an Eclipse Ci-L microscope (Nikon, Japan) installed with an Intensilight C-HGFI fluorescent lamp (Nikon, Japan) with excitation and emission filters of 495 nm and 519 nm, respectively.

Electron transport system activity

A 1-mL mixed liquor sample was collected in a 50-mL centrifuge tube, mixed with 2-mL Tris-HCl (pH 8) and 1.5 mL of 0.2% (w/v) iodonitrotetrazolium chloride solution, and placed in a shaking incubator (200 rpm, 37°C) for 30 min in the dark. After adding 1 mL of 37% (w/v) formaldehyde solution, the incubated mixture was pelleted by centrifugation (5,000 *g* for 5 min) solution, then treated with 5 mL of 99.9% methanol for 10 min in a shaking incubator (200 rpm, 37°C) in the dark. The obtained extract was filtrated through a 0.45-μm pore filter and measured for the reduced iodonitrotetrazolium formazan by absorbance at 485 nm. The ETS activity of a sample was determined using the following equation:[31]

$$U = \frac{D_{485} \times V_e}{K \times V \times t} \quad \text{(Equation 1)}$$

where U is the ETS activity (μg/mL·min), D_{485} is the absorbance at 485 nm, V_e is the volume of extract (mL), K is the slope of the standard curve, V is the sample volume (mL) and t is the incubation time (min). The standard curve was constructed using a series of methanol solutions of iodonitrotetrazolium formazan (5–30 μg/mL).

Cyclic voltammetry

CV was conducted to probe the redox reactions occurring in the reactors, using a three-electrode single-chamber electrochemical cell as previously described.[12] Two CV cells with a working volume of 225 mL were inoculated with the RM1 sludge collected during Days 61–70 (Phase M0) and 551–552 (Phase M20), respectively, at a ratio of 33% (v/v). The remaining volume was filled with a medium containing sodium acetate (5 g COD/L), sodium sulfate (0.35 g/L), and phosphate buffer (78 mM KH_2PO_4/K_2HPO_4, pH 7). The experimental CV cell was then supplemented with 20 mM of magnetite and incubated at 37°C after purging with N_2 gas for 10 min. After 24 h of incubation, CV was measured at a scan rate of 30 mV/s in the potential range from –0.8 to 0.8 V (vs. Ag/AgCl) using a potentiostat (WMPG1000S, WonATech, Korea).

Scanning electron microscopy

The morphology and microstructure of reactor sludge were characterized by scanning electron microscope (SEM). Mixed liquor samples (20 mL) taken from the reactors were washed three times and pelleted with 0.1-M phosphate buffer saline (PBS; pH 7.4) by centrifugation (2,000 *g*, 10 min), after which they were fixed

with 2.5% (w/v) glutaraldehyde in 0.1-M PBS (pH 7.4) at 4°C for 4 h. The fixed pellet was washed by centrifugation in the same manner as above, followed by serial dehydration in 50, 70, 90 and 100% (v/v) ethanol solutions (15 min each) and air-drying. The prepared specimen was loaded on an SEM stub with carbon tape, sputter-coated with platinum and characterised using a field-emission SEM system (NanoSEM 230, FEI, USA).

Microbial community analysis

The mixed liquor samples (1 mL) for total RNA extraction were pelleted by centrifugation (13000 *g*, 3 min) and resuspended in the same volume of DNA/RNA Shield (Zymo Research, USA). Total RNA was extracted from 5 μL of the resulting suspension and reverse-transcribed to cDNA using the SuperPrep Cell Lysis & RT Kit for qPCR (TOYOBO, Japan) according to the manufacturer's instructions. The cDNA libraries of bacterial and archaeal 16S rRNA for HTS analysis were prepared by polymerase chain reaction (PCR) with universal prokaryotic primers 515F and 806R, as previously described.[12] The amplified PCR products were sent to Macrogen, Inc. (Korea) for purification and sequencing on the Illumina MiSeq platform. Reads with low quality scores, ambiguous bases or potential chimeric sequences were discarded. The qualified reads were aligned and clustered using CD-HIT-OTU (http://weizhongli-lab.org/cd-hit-otu/) with an OTU cut-off of 3% sequence dissimilarity. Taxonomic classification of OTUs was made against the RDP database using the UCLUST tool[73] in the QIIME suite (ver 1.8.0).[74] The sequence data generated in this study have been deposited in the NCBI Sequence Read Archive under BioProject accession number PRJNA666182.

Pearson correlations among microbial OTUs (based on their relative abundances in each bacterial or archaeal library) and physicochemical parameters were analyzed using PAST ver. 4.03 (https://www.nhm.uio.no/english/research/infrastructure/past/). A correlation network (p <0.10) was generated from the resulting correlation matrix (r and p values) using Cytoscape ver. 3.8.1 (https://cytoscape.org/). The initial positions of the nodes were determined by a force-directed layout algorithm.

DNA stable-isotope probing and digital PCR

After the semi-continuous culture experiments described above, the quadruple bottles of C cultures were split into duplicate SC and SM cultures for DNA-SIP analysis. All bottles were fed at a 20-day HRT with a 9:1 (v/v) mixture of the reactor feed and a 78-mM $NaH^{13}CO_3$ solution. Magnetite (20 mM Fe) was continuously added to SM cultures, but not to SC cultures (control). The cultures were incubated in an anaerobic chamber as described above for C cultures. Total DNA was extracted from the mixed liquor collected during Days 55–65 from each bottle using an ExiProgen automated nucleic acid extractor (Bioneer, Korea) as previously described.[12] The purified DNA was dissolved in a gradient buffer (10 mM Tris-HCl [pH 8], 1 mM EDTA) to 5 μg/mL in a 15-mL conical tube and then mixed with 1 g of CsCl and 25 μL of 10,000× SYBR safe dye.[75] After loading the resulting mixture into 5.1-mL Quick-Seal tubes (Beckman Coulter, Germany), the remaining volume was filled with 1 g/mL CsCl solution. The tubes were heat-sealed and ultracentrifuged at 180,000 *g* at 20°C for 60 h. The light (^{12}C) and heavy (^{13}C) DNA fractions were visualized under blue light and separately retrieved using a needle and syringe.

The retrieved light and heavy DNA fractions were purified and analyzed for the 16S rRNA gene concentrations of total archaea and *Methanothrix* by dPCR using published primers/probe sets.[76] The template DNA for dPCR was quantified using the Qubit dsDNA BR Assay kit in a Qubit 2.0 Fluorometer (Life Technologies, USA). The dPCR reactions were prepared using the QIAcuity Probe PCR kit (QIAGEN, Germany) following the manufacturer's instructions and loaded onto the QIAcuity Nanoplate 26K 24-well, which can run 24 samples with up to 26,000 partitions (i.e. individual reactions) per well. The dPCR reactions were amplified and analyzed in a QIAcuity ONE 2-Plex system (QIAGEN, Germany) with the following thermal cycling profile: an initial heat activation at 95°C for 2 min and 40 cycles of amplification (denaturation at 95°C for 15 s followed by combined annealing and extension at 60°C for 30 s). A non-template control was included in each dPCR run to determine the signal-to-noise threshold. The absolute number of target genes in a sample was estimated from the fraction of positive partitions (i.e. amplified reactions) using Poisson statistics.

Other analytical methods

Solids were measured following the procedures in Standard Methods for the Examination of Water and Wastewater.[77] COD and TDS were measured using HS-COD-MR and HS-S kits (HUMAS, Korea),

respectively. VFAs (C_2–C_7) were quantified using a 7820A gas chromatograph (Agilent, USA) equipped with a flame ionisation detector and an Innowax column (Agilent, USA). Samples for measuring soluble COD and VFAs were filtered through a 0.45-μm pore syringe filter. FeS was measured by the HCl extraction method as previously described.[78] The contents of organic C, H, O, N and S were determined on a volatile solids basis using a Flash 2000 elemental analyzer (Thermo Scientific, The Netherlands). XRD analysis was performed using a D/Max2500 diffractometer (Rigaku, Japan) installed with an ultra 18kW Cu rotating-anode X-ray source. The magnetite concentration in mixed liquor was measured by a modified oxalate extraction method as described previously.[54] Biogas produced from each reactor was collected in a 10-L Tedlar bag connected to the gas outlet. The collected biogas volume was measured by water displacement and corrected to the standard temperature and pressure (0°C and 1 bar). Biogas composition (CH_4, CO_2, H_2 and H_2S) was analyzed using a 490 Micro GC System (Agilent, USA) installed with two thermal conductivity detectors fitted with a CP-Molsieve 5Å column and a CP-PoraPLOT U column (Agilent, USA), respectively. All analyses were performed at least in duplicate.

QUANTIFICATION AND STATISTICAL ANALYSIS

Statistical significance of all data was evaluated by p value < 0.05 through analysis of variance (ANOVA) using Excel.